Journal of Sound and Vibration (1999) **221**(5), 867–885
Article No. jsvi.1998.2037, available online at http://www.idealibrary.com on IDEAL

DAMPED VIBRATION OF COMPOSITE PLATES WITH PASSIVE PIEZOELECTRIC-RESISTOR ELEMENTS

D. A. SARAVANOS
Ohio Aerospace Institute, 22800 *Cedar Point Rd*., *Cleveland*, *OH* 44142, *U.S.A.*

(*Received* 1 *June* 1998, *and in final form* 9 *November* 1998)

Mechanics for the analysis of damping in composite plates with multiple resistively shunted piezoelectric layers are developed. The mixed field piezoelectric laminate theory is extended to include distributed passive electric circuitry embedded or attached to piezoelectric layers. The equations of motion for the coupled laminate/circuitry system are formulated and exactly solved for the case of simply-supported plates. The modal frequencies and damping are directly calculated from the complex eigenvalues of the damped plate. The forced vibration of the damped piezoelectric composite plate is also directly predicted. Numerical results for a cross-ply graphite/epoxy plate with surface mounted resistively shunted piezoceramic layers are presented. The results show that for each mode there is an optimal resistance value which adds significant modal damping. Away from this optimal value the modal damping gradually reduces to zero. Simultaneous shifting of the corresponding modal frequency to a higher value occurs over this optimal resistance range. The calculated frequency response of the damped plate illustrates that substantial vibration control of select modes can be obtained by proper tuning of the shunting resistive circuit.

1. INTRODUCTION

The continuous requirements imposed on many new structural applications for improved vibroacoustic response and weight reduction mandate the development of new damped structural concepts and damping mechanisms. One such possibility is the development of composite structures passively damped via embedded piezoelectric elements. Piezoelectric layers introduce the unique capability to convert strain and/or kinetic energy to electric energy during a vibration cycle and vice versa, thus enabling the dissipation of electric energy through passive electric circuitry (i.e., shunt resistors). Compared to other techniques which typically introduce high damping, such as constrained interlaminar viscoelastic layers or active damping with feedback control, the concept of passive piezoelectric damping exhibits some very desirable characteristics, such as: the level of damping may be spontaneously or periodically modified, by varying the properties of the passive electric elements

0022–460X/99/150867 + 19 $30.00/0

(resistors, capacitors, etc.) or by reconfiguring the electric circuitry; the damping improvement does not reduce the stiffness of the laminate, as is the case with shear viscoelastic damping layers; and the technique requires minimal hardware which may even be encapsulated into the laminate, thus adding minimal weight to the structure. Consequently, the approach may be very suitable for damping vibrations in rotating or moving components, such as turbomachinery blades, helicopter blades, and so forth.

While substantial work has been reported in the area of active piezoelectric damping, as summarized in recent reviews by Crawley [1] and Rao and Sunar [2], most of the reported work on passive piezoelectric damping has been limited to simple laminate and structural (mostly beam) configurations. Hagood and Von Flotow [3] first studied the use of passive piezoelectric elements to dampen beam structures. Law *et al*. [4] have reported simplified models and experimental results for piezoelectric materials shunted by a load resistor. Davis and Lesieutre [5] developed a method for predicting the passive damping in beams with resistively shunted piezoelectric patches based on the strain energy dissipation approach, and reported experimental results. Koshigoe and Murdock [6] reported a simplified analytical formulation for plates with passive piezoelectric elements. Wang *et al*. [7] reported work on a semi-active vibration control approach for beams with piezoelectric elements combining passive electric components with an active controller concept. Yarlagadda *et al*. [8] presented micromechanics and experimental results for composites with resistively shunted piezoceramic fibers.

Although the previous work has provided valuable insight into the effectiveness of the technique, development of efficient methodologies enabling analysis of more complex laminate and structural configurations seems to be required. The present paper presents a coupled electromechanical theory for composite laminates with multiple piezoelectric layers connected to passive electric circuits, and a Ritz solution for predicting the modal damping, modal frequencies and damped response of composite piezoelectric plates. The laminate mechanics combine single-layer kinematic assumptions for the displacements with a layerwise variation of the electric potential. The formulation considers the presence of distributed passive electric components embedded or attached to the piezoelectric layers, thus enabling coupled and efficient representations of the integrated laminate–electric circuit system. Governing equations of motion are developed and solved in state–space form for simply supported plates. The complex eigenvalues are calculated and used to evaluate the modal damping and frequencies of the plate. The frequency response of the damped plate is also directly calculated from the equations of motion.

2. PIEZOLAMINATES WITH PASSIVE ELECTRIC CIRCUITRY

2.1. GOVERNING MATERIAL EQUATIONS

This section describes the theoretical foundation for piezoelectric-composite laminates (identified for brevity with the term piezolaminates) having arbitrary

configurations of piezoelectric layers and composite plies, as shown schematically in Figure 1. Each piezoelectric layer may be either connected to a passive electric circuit containing resistors, capacitors and inductors, or may have an electric potential applied. A Cartesian co-ordinate system $O\xi\eta\zeta$ is defined, such that the axes ξ and η lie on the mid-plane A_o, while the axis ζ is perpendicular to the plane of the laminate. Each ply is generally assumed to consist of a linear piezoelectric material with constitutive equations of the form

$$\sigma_i = C_{ij}^E S_j - e_{ik} E_k, \quad D_l = e_{lj} S_j + \varepsilon_{lk}^S E_k, \tag{1}$$

where $i, j = 1, \ldots, 6$ and $k, l = 1, \ldots, 3$; σ_i and S_i are the mechanical stresses and engineering strains in vectorial notation; E_k is the electric field vector; D_l is the electric displacement vector; C_{ij} is the elastic stiffness tensor; e_{ij} is the piezoelectric tensor; and ε_{lk} is the electric permittivity tensor of the material. Superscripts E and S indicate constant electric field and strain conditions, respectively. The axes 1, 2, and 3 of the material are parallel to the Cartesian co-ordinate axes ξ, η, ζ, respectively.

The strain–displacement and electric field–potential relationships are

$$S_{ij} = 1/2(u_{i,j} + u_{j,i}), \quad E_k = -\phi_{,k}, \tag{2}$$

where u, v, w are the displacements, and ϕ is the electric potential.

The equations of motion consist of the stress equilibrium equations

$$\sigma_{ij,j} - \rho \ddot{u}_i = 0 \tag{3}$$

and the electric displacement equilibrium equation [9]

$$D_{i,i} = q_e, \tag{4}$$

where q_e represents the specific charge from distributed electric sources.

2.2. LAMINATE THEORY

A typical configuration of a piezolaminate with an arbitrary number of piezoelectric layers connected to distributed electric circuits is shown in

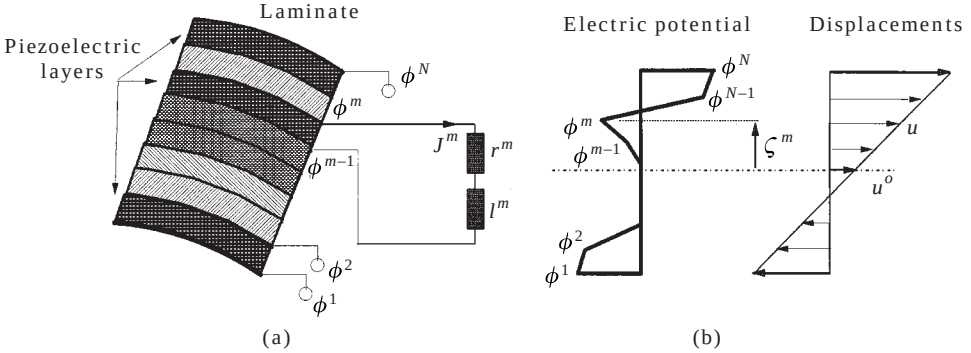

Figure 1. Piezoelectric laminate with passive electric circuitry: (a) typical configuration, (b) assumed fields for electric potential and in-plane displacements.

Figure 1(a). Some of the elements of the electric circuits may be embedded or integrated into the laminate. The theoretical framework of the so called mixed-field piezoelectric laminate theory [10] provided the basis for the mechanics of piezoelectric laminates with distributed passive electric components. The theory utilizes both displacements and electric potential as generalized state variables, yet, it combines different types of through-the-thickness approximations of the state variables. Specifically, linear displacement fields are assumed for the displacements u, v, while a layerwise electric potential field is considered through the laminate consisting of N discrete continuous segments (Figure 1(b)). Previous work [10, 11] has shown that such kinematic assumptions can capture the electric heterogeneity through-the-thickness induced by the embedded piezoelectric layers, and will accurate model thin and/or moderately thick piezoelectric shell laminates with minimal computational cost. The displacements and electric potential of the mixed-field theory take the form

$$\begin{aligned} &u(\xi,\eta,\zeta,t) = u^o(\xi,\eta,t) + \zeta\beta_x(\xi,\eta,t), \qquad v(\xi,\eta,\zeta,t) = v^o(\xi,\eta,t) + \zeta\beta_y(\xi,\eta,t), \\ &w(\xi,\eta,\zeta,t) = w^o(\xi,\eta,t), \qquad \phi(\xi,\eta,\zeta,t) = \sum_{j=1}^{N} \phi^j(\xi,\eta,t)\Psi^j(\zeta), \end{aligned} \tag{5}$$

where u^o, v^o, w^o are displacements on mid-surface; superscript j indicates the points ζ^j at the beginning and end of each discrete layer; ϕ^j is the electric potential at each point ζ^j (see Figure 1); $\Psi^j(\zeta)$ are interpolation functions; and β_ξ, β_η are the rotation angles. In the context of equation (5), the engineering strains become

$$S_i(\xi,\eta,\zeta,t) = S_i^o(\xi,\eta,t) + \zeta k_i(\xi,\eta,t), \quad i = 1, 2, 6; \quad S_3(\xi,\eta,\zeta,t) = 0;$$

$$S_i(\xi,\eta,\zeta,t) = S_i^o(\xi,\eta,t), \quad i = 4, 5; \tag{6}$$

where S^o and k are the strain and curvature vectors at the reference surface. The electric field vector also becomes

$$\begin{aligned} E_i(\xi,\eta,\zeta,t) &= \sum_{j=1}^{N} E_i^j(\xi,\eta,t)\Psi^j(\zeta), \quad i = 1, 2; \\ E_3(\xi,\eta,\zeta,t) &= \sum_{j=1}^{N} E_3^j(\xi,\eta,t)\Psi^j{}_{,\zeta}(\zeta), \end{aligned} \tag{7}$$

where $\{E^j\}$ is the generalized electric field vector defined as

$$E_1^j = -\phi^j{}_{,\xi}, \quad E_2^j = -\phi^j{}_{,\eta}, \quad E_3^j = -\phi^j. \tag{8}$$

2.2.1. *Equations of motion*

The laminate equations of motion are derived by integrating equations (3, 4) through-the-thickness of the laminate in terms of generalized forces

$$N_{1,\xi} + N_{6,\eta} - (\rho^A \ddot{u}^o + \rho^B \ddot{\beta}_\xi) = -q_5,$$
$$N_{6,\xi} + N_{2,\eta} - (\rho^A \ddot{v}^o + \rho^B \ddot{\beta}_\eta) = -q_4, \quad N_{5,\xi} + N_{4,\eta} - \rho^A \ddot{w}^o = -q_3, \tag{9}$$

generalized moments

$$M_{1,\xi} + M_{6,\eta} - N_5 - (\rho^B \ddot{u}^o + \rho^D \ddot{\beta}_\xi) = -p_5,$$
$$M_{6,\xi} + M_{2,\eta} - N_4 - (\rho^B \ddot{v}^o + \rho^D \ddot{\beta}_\eta) = -p_4, \tag{10}$$

and the rate of change of generalized electric charges

$$\dot{D}^m_{1,\xi} + \dot{D}^m_{2,\eta} - \dot{D}^m_3 = -\bar{J}^m_3, \quad m = 1, \ldots, N, \tag{11}$$

where q and p indicate surface tractions and moments, respectively; subscripts 4, 5 indicate shear and subscripts 1, 2, 3 normal components; $\bar{J}^m_3$ is the electric flux along the thickness direction at point ζ^m, usually corresponding to an electrode surface. The resultant forces N_i, M_i and electric displacements D^m_i are defined and related to the generalized strain and electric field of the piezoelectric laminate as follows:

$$N_i = \int_0^h \sigma_i \, \mathrm{d}\zeta = A_{ij} S^o_j + B_{ij} k_j - \sum_{m=1}^N \bar{E}^m_{3i} E^m_3, \quad i, j = 1, 2, 6,$$
$$N_i = \int_0^h \sigma_i \, \mathrm{d}\zeta = A_{ij} S^o_j - \sum_{m=1}^N \bar{E}^m_{ik} E^m_k, \quad i, j = 4, 5, \quad k = 1, 2, \tag{12}$$
$$M_i = \int_0^h \sigma_i \zeta \, \mathrm{d}\zeta = B_{ij} S^0_j + D_{ij} k_j - \sum_{m=1}^N \hat{E}^m_{3i} E^m_3, \quad i, j = 1, 2, 6,$$

$$D^m_i = \int_o^h \langle D_1, D_2 \rangle \Psi^m(\zeta) \, \mathrm{d}\zeta = \bar{E}^m_{ij} S^o_j + \sum_{n=1}^N G^{mn}_{ii} E^n_i, \quad i = 1, 2, \quad j = 4, 5,$$
$$D^m_3 = \int_0^h D_3 \Psi^m_{,\zeta}(\zeta) \, \mathrm{d}\zeta = \bar{E}_{3j} S^o_j + \hat{E}_{3j} k_j + \sum_{n=1}^N G^{mn}_{33} E^n_3, \quad j = 1, 2, 6. \tag{13}$$

In the above equations, $[A]$, $[B]$, and $[D]$ are the stiffness matrices of the laminate, $[\bar{E}^m]$ and $[\hat{E}^m]$ are the piezoelectric laminate matrices, $[G^{mn}]$ are the laminate matrices of electric permittivity, and ρ^A, ρ^B, ρ^D are the generalized densities, expressing the mass, mass coupling and rotational inertia per unit area, of the laminate, respectively. The definitions of all laminate matrices are shown in Appendix A.

Considering a configuration of passive circuits with resistive and inductive elements interfaced to the terminal surfaces (Figure 1(a)) of piezoelectric layers, the electric potential $\{\phi^p\}$ and electric flux $\{J^p\}$ in the circuitry are related by the Kirchoff's law

$$\phi^P(t) = [r]J^P(t) + [l]\dot{J}^P(t), \tag{14}$$

where $[r]$ and $[l]$ are resistance and inductance matrices per unit area of the laminate. If an electric circuit is connected to the laminate at point ζ^m, the compatibility conditions at this interface require that the electric potentials are equal and the electric flux between the laminate and the circuit is preserved

$$\phi^m = \phi^P, \quad \bar{J}_3^m = J^P. \tag{15}$$

3. LAMINATED PIEZOELECTRIC PLATES

An exact solution of the governing equations (9)–(11) was developed for simply-supported rectangular plates with orthotropic composite plies and piezoelectric layers polarized along the thickness direction ($C_{16} = C_{26} = e_{36} = 0$). Axes ξ, η are assumed parallel to the sides of the plate. Equations (9, 10) for the balance of forces and moments yield five differential equations of the form:

$$A_{11}S^o_{1,\xi} + A_{12}S^o_{2,\xi} + B_{11}k_{1,\xi} + B_{12}k_{2,\xi} + A_{66}S^o_{6,\eta} + B_{66}k_{6,\eta} - \sum_{m=1}^{N} \bar{E}^m_{31}E^m_{3,\xi}$$

$$-(\rho^A \ddot{u}^o + \rho^B \ddot{\beta}_\xi) = -q^5,$$

$$A_{66}S^o_{6,\xi} + B_{66}k_{6,\xi} + A_{21}S^o_{1,\eta} + A_{22}S^o_{2,\eta} + B_{21}k_{1,\eta} + B_{22}k_{2,\eta} - \sum_{m=1}^{N} \bar{E}^m_{32}E^m_{3,\eta}$$

$$-(\rho^A \ddot{v}^o + \rho^B \ddot{\beta}_\eta) = -q^4,$$

$$A_{55}S^o_{5,\xi} - \sum_{m=1}^{N} \bar{E}^m_{15}E^m_{1,\xi} + A_{44}S^o_{4,\eta} - \sum_{m=1}^{N} \bar{E}^m_{24}E^m_{2,\eta} - \rho^A \ddot{w}^o = -q^3, \tag{16}$$

$$B_{11}S^0_{1,\xi} + B_{12}S^o_{2,\xi} + D_{11}k_{1,\xi} + D_{12}k_{2,\xi} + B_{66}S^o_{6,\eta} + D_{66}k_{6,\eta} - \sum_{m=1}^{N} \hat{E}^m_{31}E^m_{3,\xi}$$

$$-(\rho^B \ddot{u}^o + \rho^D \ddot{\beta}_\xi) = -p^5,$$

$$B_{66}S^o_{6,\xi} + D_{66}k_{6,\xi} + B_{21}S^o_{1,\eta} + B_{22}S^o_{2,\eta} + D_{21}k_{1,\eta} + D_{22}k_{2,\eta} - \sum_{m=1}^{N} \hat{E}^m_{32}E^m_{3,\eta}$$

$$-(\rho^B \ddot{v}^o + \rho^D \ddot{\beta}_\eta) = -p^4,$$

while the generalized charge conservation equation (11), may yield N additional

equations:

$$\bar{E}^n_{15}\dot{S}^o_{5,\xi} + \sum_{m=1}^{N} G^{nm}_{11}\dot{E}^m_{1,\xi} + \bar{E}^n_{24}\dot{S}^o_{4,\eta} + \sum_{m=1}^{N} G^{nm}_{22}\dot{E}^m_{2,\eta}$$

$$-(\bar{E}^n_{31}\dot{S}^o_1 + \bar{E}^n_{32}\dot{S}^o_2 + \hat{E}^n_{31}\dot{k}_1 + \hat{E}^n_{32}\dot{k}_2 + \sum_{m=1}^{N} G^{nm}_{33}\dot{E}^m_3) = -\bar{J}^n_3, \quad n = 1, \ldots, N. \quad (17)$$

Incorporating equations (5, 6, 8) into equations (16, 17), a coupled system of $N + 5$ differential equations with $N + 5$ unknowns results. The boundary conditions for a simply supported piezoelectric plate are: $v^o(\xi, 0) = (v^o(\xi\ L_\eta) = u^o(0, \eta) = u^o(L_\xi, \eta) = w^o(\xi, 0) = w^o(\xi, L_\eta) = w^o(0, \eta) = w^o(L_\xi, \eta) = 0$ and $\phi^j(\xi, 0) = \phi^j(\xi, L_\eta) = \phi^j(0, \eta) = \phi^j(L_\xi, \eta) = 0$. A fundamental set of mode shapes satisfying the boundary conditions is

$$\begin{aligned}
&u^o(\xi,\eta,t) = U^o_{kl}(t)\cos(a\xi)\sin(b\eta), \quad v^o(\xi,\eta,t) = V^o_{kl}(t)\sin(a\xi)\cos(b\eta),\\
&w^o(\xi,\eta,t) = V^0_{kl}(t)\sin(a\xi)\sin(b\eta),\\
&\beta_\xi(\xi,\eta,t) = \beta_{\xi kl}(t)\cos(a\xi)\sin(b\eta), \quad \beta_\eta(\xi,\eta,t) = \beta_{\eta kl}(t)\sin(a\xi)\cos(b\eta),\\
&\phi^j(\xi,\eta,t) = \Phi^j_{kl}(t)\sin(a\xi)\sin(b\eta), \quad a = k\pi/L_\xi, \quad b = l\pi/L_\eta,
\end{aligned} \quad (18)$$

where L_ξ, L_η are the dimensions of the plate and k, $l = 1, 2, 3, \ldots$ are the number of semi-wavelengths along the ξ and η directions of the respective mode, indicated as mode (k, l). For example, substitution of $k = 1$ and $l = 1$ into equations (18) yields the fundamental mode shape (1, 1); $k = 2$, $l = 1$ yields the mode shape (2, 1) with a modal line ($w = 0$) along $\xi = L_\xi/2$; $k = 1$, $l = 2$ yields the mode shape (1, 2) with a modal line ($w = 0$) along $\eta = L_\eta/2$ and so forth.

Substituting the fundamental solution (18) into the generalized equations of motion (16, 17) the following linear system of $N + 5$ dynamic equations results for each $\{k, l\}$ vibration mode of the plate:

$$(a^2A_{11} + b^2A_{66})U^o_{kl} + ab(A_{12} + A_{66})V^o_{kl} + (a^2B_{11} + b^2B_{66})\beta_{\xi_{kl}} + ab(B_{12} + B_{66})\beta_{\eta_{kl}}$$

$$-\sum_{m=1}^{N} a\bar{E}^m_{31}\Phi^m_{kl} + (\rho^A\ddot{U}^o_{kl} + \rho^B\ddot{\beta}_{\xi_{kl}}) = q^5_{kl},$$

$$ab(A_{12} + A_{66})U^o_{kl} + (b^2A_{22} + a^2A_{66})V^o_{kl} + ab(B_{12} + B_{66})\beta_{\xi_{kl}} + (b^2B_{22} + a^2B_{66})\beta_{n_{kl}}$$

$$-\sum_{m=1}^{N} b\bar{E}^m_{32}\Phi^m_{kl} + (\rho^A\ddot{V}^o_{kl} + \rho^B\ddot{\beta}_{n_{kl}}) = q^4_{kl},$$

$$(a^2A_{55} + b^2A_{44})W^o_{kl} + aA_{55}\beta_{\xi_{kl}} + bA_{44}\beta_{\eta_{kl}} + \sum_{m=1}^{N}(a^2\bar{E}^m_{15} + b^2\bar{E}^m_{24})\Phi^m_{kl} + \rho^4\ddot{W}^o_{kl} = q^3_{kl},$$

$$(a^2B_{11}+b^2B_{66})U^o_{kl}+ab(B_{12}+B_{66})V^o_{kl}+(a^2D_{11}+b^2D_{66})\beta_{\xi_{kl}}+ab(D_{12}+D_{66})\beta_{\eta_{kl}}$$
$$-\sum_{m=1}^{N}a\hat{E}^m_{31}\Phi^m_{kl}+(\rho^B\ddot{U}^o_{kl}+\rho^D\ddot{\beta}_{\xi_{kl}})=p^5_{kl},$$

$$ab(B_{12}+B_{66})U^o_{kl}+(b^2B_{22}+a^2B_{66})V^o_{kl}+ab(D_{12}+D_{66})\beta_{\xi_{kl}}+(b^2D_{22}+a^2D_{66})B_{n_{kl}}$$
$$-\sum_{m=1}^{N}b\hat{E}^m_{32}\Phi^m_{kl}+(\rho^B\ddot{V}^o_{kl}+\rho^D\ddot{\beta}_{\eta_{kl}})=p^4_{kl},$$

$$a\bar{E}^n_{31}\dot{U}^o_{kl}+b\bar{E}^n_{32}\dot{V}^o_{kl}-(a^2\bar{E}^n_{15}+b^2\bar{E}^n_{24})\dot{W}^o_{kl}-a(\bar{E}^n_{15}+\hat{E}^n_{31})\dot{\beta}_{\eta_{kl}}-b(\bar{E}^n_{24}+\hat{E}^n_{32})\dot{\beta}_{\eta_{kl}}$$
$$+\sum_{m=1}^{N}(-a^2G^{nm}_{11}-b^2G^{nm}_{22}+G^{nm}_{33})\dot{\Phi}^m_{kl})=\bar{J}^n_{3kl},\quad n=1,\ldots,N. \tag{19}$$

Considering an active–passive laminate, with N_p piezoelectric layers connected to passive circuitry while the remaining piezoelectric layers are configured as actuators (electric potential applied on both surfaces), the electric potential vector can be subdivided into a passive component Φ^p representing the electric output at passive piezoelectric layers and a forced or active component Φ^A representing the voltage imposed on the active layers, such that $\{\Phi\}=\{\Phi^P;\ \Phi^A\}$. Collecting the coefficients in equation (19) and separating the passive and active electric potential components, the system of dynamic equations is reduced to the following $5+N_p$ equations, which can be written in matrix form:

$$[M_{uu}]\{\ddot{U}_{kl}\}+[K_{uu}]\{U_{kl}\}+[K^{PP}_{u\phi}]\{\Phi^P_{kl}\}=\{F_{kl}(t)\}-[K^{PA}_{u\phi}]\{\Phi^A_{kl}(t)\},$$
$$[K^{PP}_{\phi u}]\{\dot{U}_{kl}\}+[K^{PP}_{\phi\phi}]\{\dot{\Phi}^P_{kl}\}-\{J^P_{3kl}(t)\}=0, \tag{20}$$

where $U=\{U^o,\ V^o,\ W^o,\ \beta_\xi,\beta_\eta\}$ and $\Phi=\{\Phi^1,\ldots,\Phi^N\}=\{\Phi^P;\ \Phi^A\}$ are the unknown gains of each vibration mode in equation (18). Submatrices K_{uu}, $K_{u\phi}$, $K_{\phi\phi}$, and M_{uu} are coefficient matrices depending on the generalized elastic, piezoelectric, permittivity and mass laminate matrices, respectively, and the mode order kl. Superscripts P and A indicate the partitioned submatrices in accordance with the selected passive and active configuration, respectively. The left-hand side includes the unknown electromechanical state $\{U;\ \Phi^p,\ J^p\}$ which contains the displacements, the electric potential and electric flux at the passive piezoelectric layers. The right-hand side includes the excitation of the plate in terms of mechanical loads and applied voltages on the actuators. The above dynamic system is combined with the equation of the passive circuitry (14) to yield the dynamic equations of the damped piezoelectric plate. Assuming a resistive circuit, the dynamic equations in state–space form are

$$\begin{bmatrix} [M_{uu}] & 0 & 0 \\ 0 & I & 0 \\ 0 & 0 & [K^{PP}_{\phi\phi}] \end{bmatrix} \begin{Bmatrix} \{\dot{V}\} \\ \{\dot{U}\} \\ \{\dot{\Phi}^p\} \end{Bmatrix} = \begin{bmatrix} 0 & -[K_{uu}] & -[K^{PP}_{u\phi}] \\ I & 0 & 0 \\ [-K^{PP}_{\phi u}] & 0 & [r]^{-1} \end{bmatrix} \begin{Bmatrix} \{V\} \\ \{U\} \\ \{\Phi^p\} \end{Bmatrix} + \begin{Bmatrix} \{F(t)\} - [K^{PA}_{u\phi}]\{\Phi^A(t)\} \\ 0 \\ 0 \end{Bmatrix}, \quad (21)$$

where subscripts kl are implied on state variables and $\{V\}$ is the rate of change of the displacement vector. This dynamic system may provide either the free vibration and/or the frequency response of the damped plate. Assuming that $\{X\} = \{U^o, V^o, W^o, \beta_\xi, \beta_\eta, \Phi^P\}$, equation (21) can be written in standard form

$$[A]\{\dot{X}_{kl}(t)\} = [B]\{X_{kl}(t)\} + \{P_{kl}(t)\}. \quad (22)$$

3.1. MODAL CHARACTERISTICS

Assuming free vibration conditions ($P = 0$) and state variables of the form $\{X_{kl}(t)\} = \{X_{kl}\}e^{st}$, equation (22) produces a generalized eigenvalue problem for each mode kl:

$$s[A]\{X\} = [B]\{X\}, \quad (23)$$

which provides $10 + N_p$ eigenvalues (poles). The first 10 poles are 5 conjugate complex pairs s^*_{kl} corresponding to one flexural, two extensional and two shear modes through the thickness of the plate. The remaining N_p eigenvalues are negative real poles corresponding to time constants of the formed electric circuitry. The modal frequency and damping ratio of the structural modes are directly calculated from the magnitude and real part of the complex poles

$$\omega_{kl} = ||s^*_{kl}||, \quad \zeta_{kl} = \mathrm{Re}(s^*_{kl})/\omega_{kl}. \quad (24)$$

3.2. FREQUENCY RESPONSE

Assuming harmonic state variables $\{X(t)\} = \{X\}e^{j\omega t}$ and harmonic force and applied electric potential $Fe^{j\omega t}$ and $\Phi^A\ e^{j\omega t}$equation (22) provides a linear system of $10 + N_p$ equations with complex coefficients:

$$(j\omega[A] - [B])\{X_{kl}\} = \{P_{kl}\}. \quad (25)$$

Solution of the system yields the complex modal amplitude X_{kl}, which represents the participation factor of the kl mode to the frequency response of the plate at any point, in the context of equation (18). The superposition of all modal amplitudes yields the response of the plate at frequency ω.

4. NUMERICAL RESULTS

A simply supported [p/0/90/90/0/p] cross-ply Graphite/Epoxy composite square plate with surface attached piezoceramic (PZT-4) or piezopolymer (PVDF) layers was modelled using the developed mechanics. The 0° plies are aligned with the ξ-axis. The damped modal characteristics of the plate and its frequency response were predicted.

The nominal thickness of each composite ply was $t_1 = 0{\cdot}375$ mm and of each piezoelectric layer was $t_p = 0{\cdot}250$ mm, thus resulting in a total plate thickness $h = 2$ mm. The free length of the plate along the ξ and η axes was $L_\xi/h = L_\eta/h = 157$. Material properties are provided in Table 1. Unless otherwise stated, both piezoelectric layers were assumed to be passively shunted, each with a resistor of equal distributed resistance per unit area r (see Figure 2). The assumed layerwise electric potential field has three linear segments ($N = 4$) with four generalized electric potential defined at the bottom and top of each piezoelectric layer, i.e., ϕ^1 at $z = -h/2$, ϕ^2 at $z = -h/2 + t_p$, ϕ^3 at $z = h/2 - t_p$ and ϕ^4 at $z = h/2$. The inner terminals of the piezoelectric layers were grounded ($\phi^2 = \phi^3 = 0$ V) while the outer terminals remained free, although connected to the resistors, leading to $\phi^p = \{\phi^1, \phi^4\}$ and $\phi^A = \{\phi^2 = 0, \phi^3 = 0\}$ V.

4.1. MODAL CHARACTERISTICS

The predicted modal frequencies and modal damping ratios of the plate with piezoceramic (PZT-4) passive layers were calculated as a function of the specific

TABLE 1

Mechanical properties ($\varepsilon_o = 8{\cdot}85 \times 10^{-12}$ farad/m · electric permittivity of air)

	Gr/Epoxy	PZT-4	PVDF
Elastic properties:			
E_{11} (GPa)	132·4	81·3	4
E_{22} (GPa)	10·8	81·3	4
E_{33} (GPa)	10·8	64·5	4
G_{23} (GPa)	3·6	25·6	1·5
G_{13} (GPa)	5·6	25·6	1·5
G_{12} (GPa)	5·6	30·6	1·5
ν_{12}	0·24	0·33	0·3
ν_{13}	0·24	0·43	0·3
ν_{23}	0·49	0·43	0·3
Piezoelectric coefficients (10^{-12} m/V):			
d_{31}	0	−122	−23
d_{32}	0	−122	−23
d_{24}	0	495	0
d_{15}	0	495	0
Electric permittivity:			
$\varepsilon_{11}/\varepsilon_o$	3·5	1475	12·4
$\varepsilon_{22}/\varepsilon_o$	3	1475	12·4
$\varepsilon_{33}/\varepsilon_o$	3	1300	12·4
Mass density ρ (kg/m^3)	1578	7600	1780

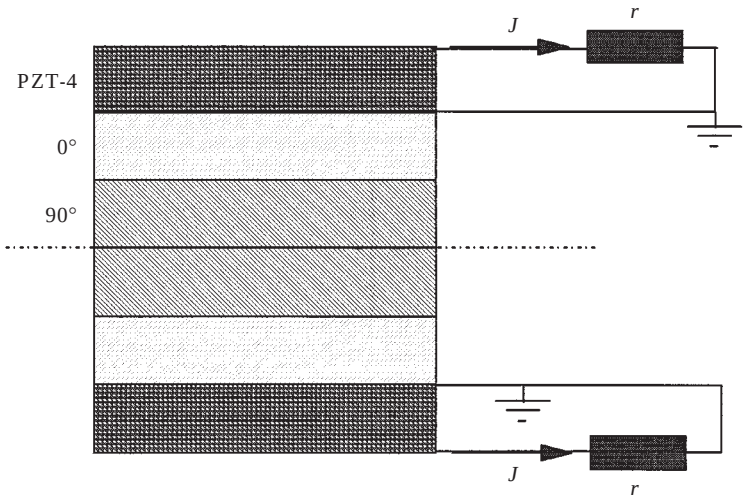

Figure 2. $[p/0/90]_s$ Laminate with two resistively shunted piezoceramic layers.

resistance r of the passive circuitry. The predicted variation of the damping ratio corresponding to the fundamental flexural mode is shown in Figure 3. The damping remains practically zero for low values of specific resistance r, because no energy is dissipated at the electric circuit and the viscoelastic material damping of the composite and piezoelectric plies was neglected. As the resistance increases, the modal damping starts to increase gradually because more electric energy is dissipated in the resistors. Interestingly, the modal damping reaches a maximum value beyond which further increase in resistance seems to lead to gradual reductions until it becomes zero for very high resistance values. In addition to this important tuning effect, the results demonstrate that significant amounts of passive piezoelectric damping may be introduced for the fundamental mode provided that a tuned resistance is used. The predicted dependence of modal damping on the shunting resistance has been experimentally observed on beam specimens by Davis and Lesieutre [5]. The resistors form a low pass filter with the capacitance of the piezoceramic layers. At the maximum damping value the cut-off frequency approaches the natural frequency of the plate allowing for maximum electric flux through the resistor. Higher resistance values gradually shift the cut-off frequency below the natural frequency of the plate and an increasing portion of electric flux is stored in the piezoelectric capacitor, thus the electric flux through the resistor and the amount of dissipated electric energy is decreased, resulting in the predicted progressive damping reduction.

It may be also observed in Figure 3 that the natural frequency remains constant at low resistance values and gradually shifts to a higher value as the resistance is increased. The corresponding modal frequency shifting occurs near the point of maximum damping. As mentioned in the previous paragraph, the shunting resistance controls what portion of the electric flux generated in the piezoelectric layers is either dissipated in the resistor or stored in the piezoelectric capacitor during a vibration cycle. As the resistance gradually increases, higher

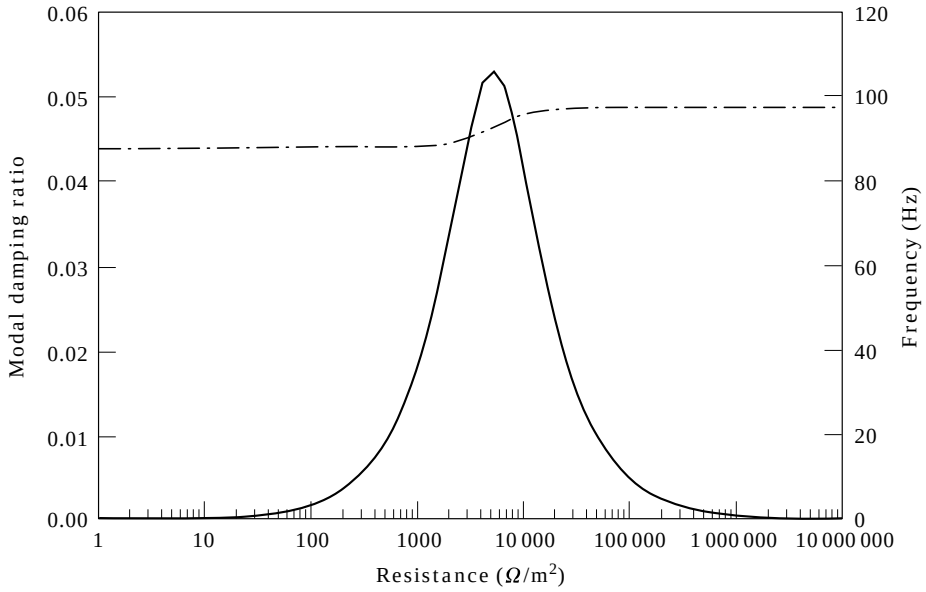

Figure 3. Effect of resistance on the modal damping and frequency of the fundamental mode (1,1). $[p/0/90]_s$ Gr/Epoxy plate with PZT-4 layers; —, modal damping; —·—, modal frequency.

portions of electric energy are either dissipated or stored, thus the elastic strain energy in the laminate is reduced and the plate stiffens. This explains why the natural frequency shifts to a higher value near the point of maximum modal damping.

The variation of the natural frequencies of the four flexural modes (1,1), (1,2), (2,1) and (2,2) is shown in Figure 4. It seems that the higher natural frequencies shift at lower resistance values. The physical explanation for this phenomenon was provided in the previous two paragraphs. Previous studies [11] on the free-vibration response of piezoelectric plates have indeed shown lower natural frequencies with closed-circuit conditions imposed on the piezelectric layers ($r \approx 0$) and higher natural frequencies with open-circuit conditions ($r \approx \infty$). These results are shown with open and closed symbols in Figure 4 and their agreement validates the natural frequency predictions of the present approach. The results illustrate that gradual variation between these extreme values is possible with resistively shunted piezoelectric laminates.

The predicted effect of shunting resistance on the modal damping of higher flexural modes (1, 2), (2, 1), (2, 2) is shown in Figure 5. It may be observed that the dependence of the modal damping of higher flexural modes to the shunting resistance was similar to the fundamental mode (1, 1). Yet, each mode reaches damping peaks which differ in value and occur at lower resistance as the mode order increases. The predicted overall dependence of natural frequency, maximum modal damping and corresponding optimal resistance values on the flexural mode order (k, l) is shown in Figure 6. Figure 6(a) shows the predicted lower and upper bounds of the modal frequencies, corresponding to zero ($r = 0$) and infinite ($r = \infty$) resistance, respectively. Figure 6(b) shows the maximum

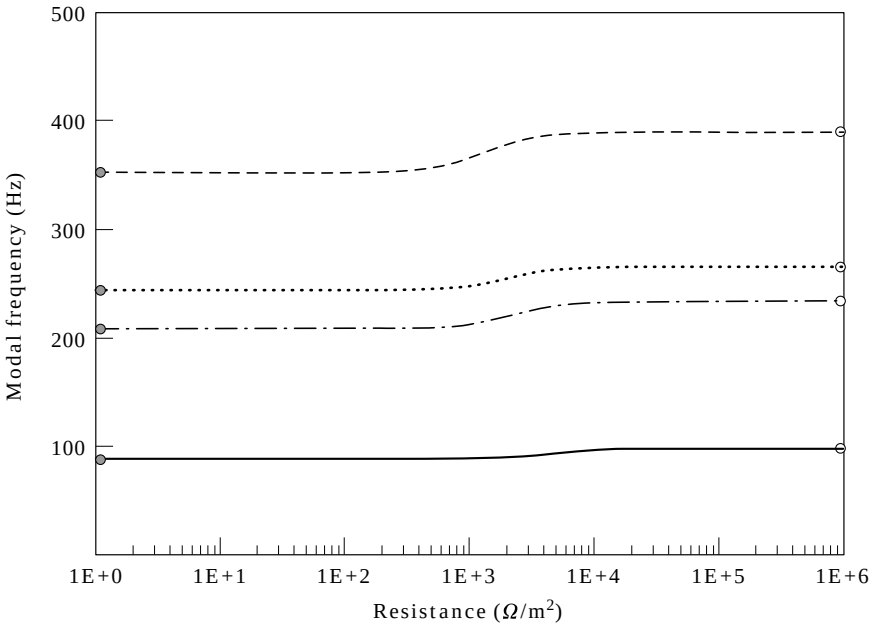

Figure 4. Effect of resistance on the modal frequencies of the $[p/0/90]_s$ plate with PZT-4 piezoceramic layers: —, mode (1,1); —·—, mode (1,2); ....., mode (2,1); ––, mode (2,2); ●, closed-circuit; ○ open-circuit.

modal damping which can be obtained with a tuned resistor for each mode, and Figure 6(c) shows the optimal resistance values which result in maximum modal damping. Figure 6(b) illustrates that at long wavelengths (low k or l) the maximum modal damping depends on the mode order. All results demonstrate

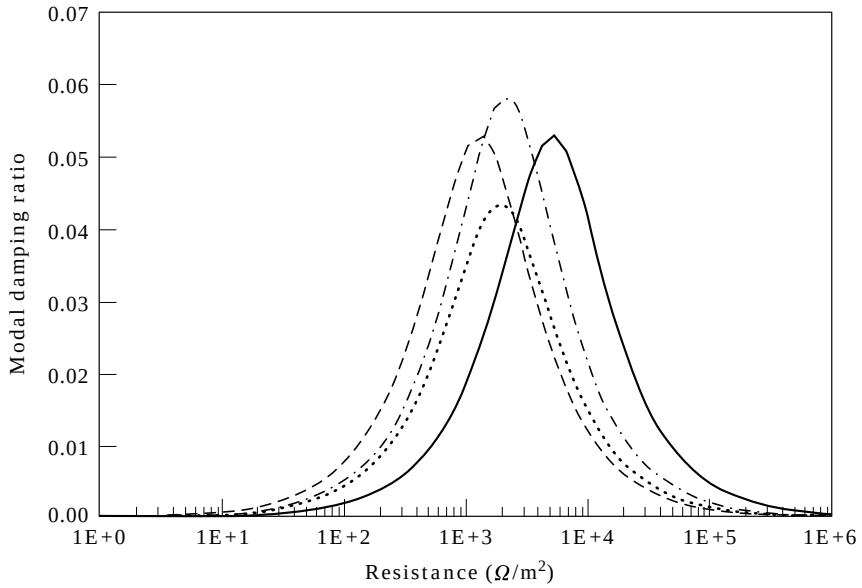

Figure 5. Effect of resistance on the modal damping of the $[p/0/90]_s$ plate with PZT-4 piezoceramic layers: —, mode (1,1); —·—, mode (1,2), ... mode (2,1); ––, mode (2,2).

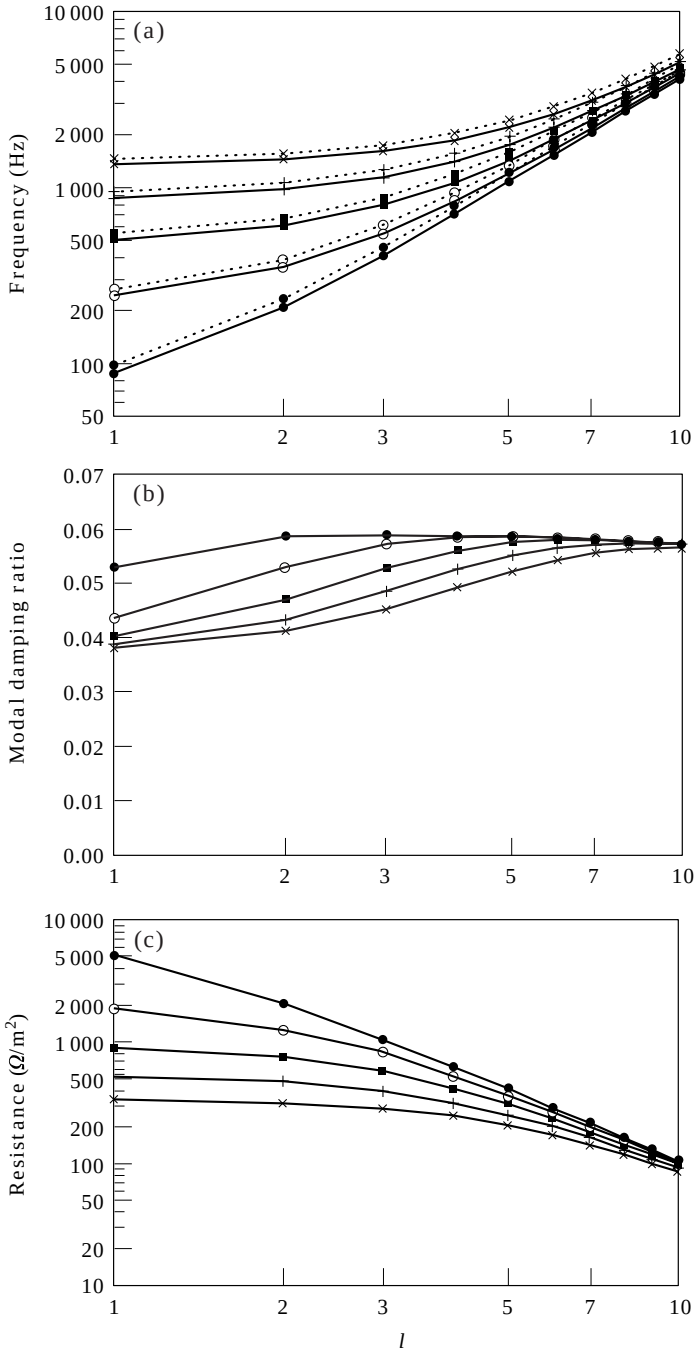

Figure 6. Dependence of modal characteristics on mode order (k, l); (a) modal frequency f_{kl} for zero and infinite resistance: —, $r = 0$; ----, $r = \infty$, Ω/m^2; (b) maximum modal damping ζ_{kl}; (c) corresponding optimal resistance r_{kl}: ●, $k = 1$; ○ $k = 2$; ■, $k = 3$; +, $k = 4$; ×, $k = 5$; $[p/0/90]_s$ plate with PZT-4 layers; k, l indicate the number of semi-wavelengths along ξ and η axes, respectively.

that significant amounts of passive piezoelectric damping may be introduced in the plate for specific modes provided that a tuned resistance is used.

4.2. FREQUENCY RESPONSE

The cumulative effect of resistively loaded piezoelectric layers on the forced vibration of the plate was also investigated for various values of passive resistance r. Figure 7 shows the frequency response of the lateral deflection w at point $(x/L_\xi, y/L_\eta) = (1/4, 1/4)$ when a harmonic uniform pressure of 1 kPa amplitude is applied over the area of the plate. Figure 7 clearly illustrates that select vibration modes can be effectively damped by changing the resistance of the circuit. The shifting of the resonance peaks is also evident. Yet, Figure 7 also depicts the difficulty of the approach to dampen all modes simultaneously. Simultaneous vibration control of many modes will require special design consideration, such as incorporation of multiple passive piezoelectric layers, each one shunted with individually tuned resistors. The value of the present mechanics in achieving such optimal design configurations is apparent.

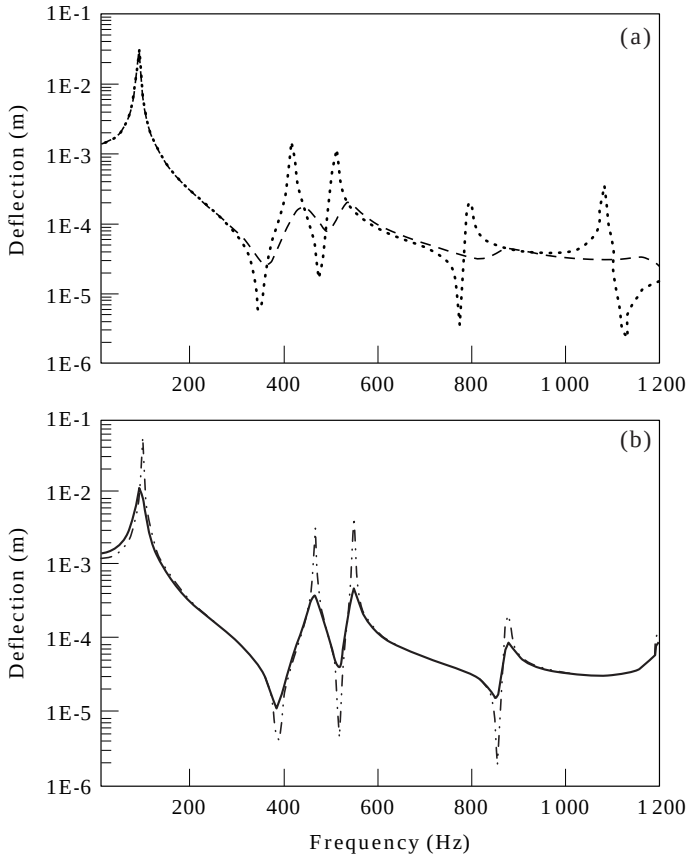

Figure 7. Frequency response functions of a square $[p/0/90]_s$, plate subject to uniform harmonic pressure for various resistance values; (a) dampening of higher modes: ----, $r = 10$; —, $r = 1000$ Ω/m^2 (b) dampening of first mode: —, $r = 5000$; — · · —, $r = 50\,000$ Ω/m^2. Deflections are at point $(\xi/L_\xi, \eta/L_\eta) = (1/4,1/4)$.

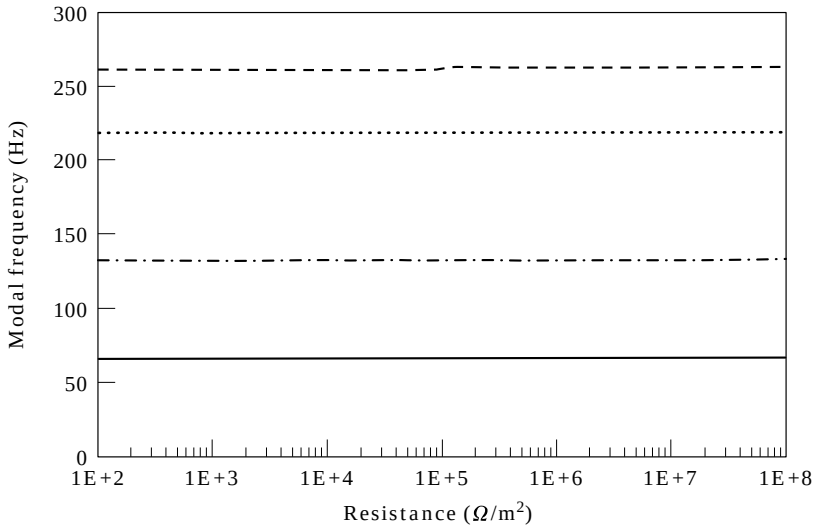

Figure 8. Effect of resistance on the modal frequencies of the $[p/0/90]_s$ plate with PVDF layers: —, mode (1, 1); — · —, mode (1, 2); . . . . . , mode (2, 1); – –, mode (2, 2).

4.3. EFFECT OF PIEZOELECTRIC MATERIAL

In addition to PZT-4 which is a hard piezoceramic material, the dynamic characteristics of the plate using a soft piezoceramic (PZT-5J) and a piezopolymer (PVDF) material were predicted to illustrate the effectiveness of various piezoelectric materials. The maximum modal damping and shifting in natural frequencies of the plate with resistively shunted PZT-5J piezoceramic layers were found to be slightly higher than the ones predicted with PZT-4, thus they are not shown. The modal frequency and damping variations for a plate

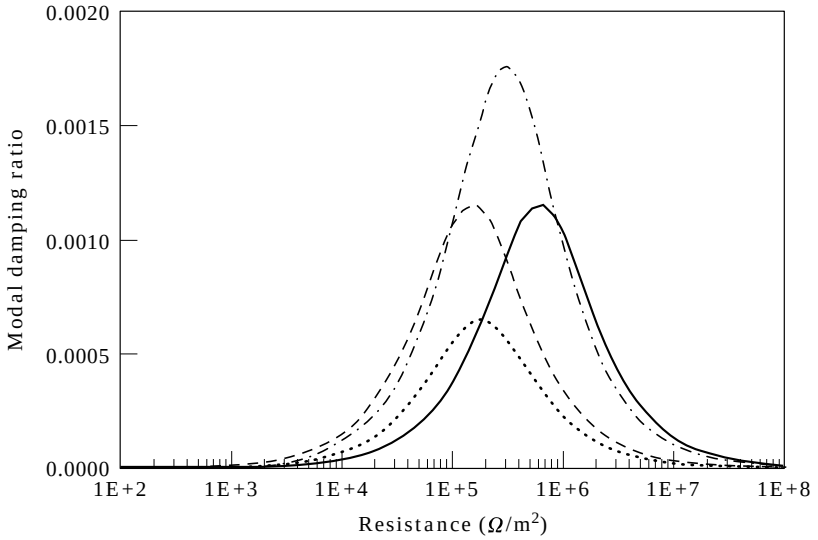

Figure 9. Effect of resistance on the modal damping of the $[p/0/90]_s$ plate with PVDF layers: —, mode (1, 1); — · —, mode (1, 2); . . . . . , mode (2, 1); – –, mode (2, 2).

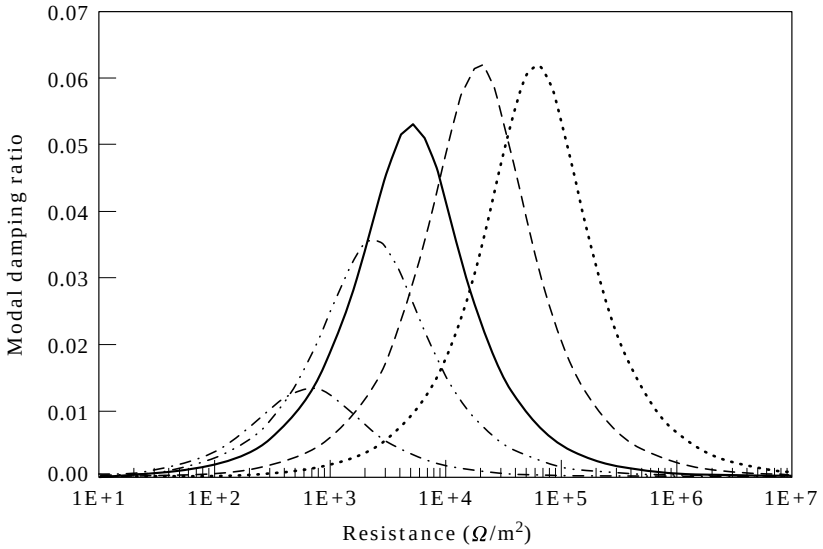

Figure 10. Effect of PZT-4 layer thickness on the fundamental damping of the $[p/0/90]_s$ plate. —·—, $t_p/10$; —··—, $t_p/2{\cdot}5$; —, t_p; – –, $5t_p$; . . . . . , $10t_p$.

with resistively loaded PVDF layers are shown in Figures 8 and 9, respectively. Clearly, much lower damping levels may be added to the structure with this piezopolymer, as a result of its substantially lower moduli and piezoelectric coefficients. The shifting in natural frequencies between low and high resistance values is rather negligible (Figure 8).

4.4. EFFECT OF PIEZOELECTRIC LAYER THICKNESS

Figure 10 shows the predicted damping of the fundamental mode for various thicknesses of PZT-4 piezoceramic layers shown as fractions of their nominal thickness $t_p = 0{\cdot}250$ mm. The maximum modal damping increases with the thickness of the piezoelectric layers until a saturation thickness is reached, beyond which the maximum damping may decrease. Significant modal damping levels may be attained even with very thin piezoceramic layers. The corresponding values of optimal resistance depend on the thickness of the piezoelectric layers, as this affects both the capacitance of the layer and the fundamental frequency of the plate.

Overall, the results indicate that significant passive damping may be added in plate structures with passive piezoceramic layers. Yet, the levels of the passive damping strongly depend on a multitude of parameters, including the resistance value, mode order, thickness and type of the piezoelectric material. Therefore, special consideration is required in the design of such damped plates including the tuning of the electric circuits. The value of the present mechanics in realizing such optimal design configurations is apparent.

5. SUMMARY

Analytical models for predicting the passive damping and damped dynamic response of active–passive composite plates with multiple resistively shunted piezoelectric layers were presented. The previously developed coupled mixed piezoelectric laminate theory was extented to include distributed passive electric circuitry embedded or attached to the piezoelectric layers. The equations of motion for such passive laminate systems were formulated and exactly solved for the case of simply-supported plates. The complex eigenvalues of the damped plate were calculated to obtain the modal frequencies and damping. The forced vibration of the plate was also calculated. Case studies on a cross–ply graphite/epoxy plate with two surface mounted resistively shunted piezoceramic patches were presented. The results show that an optimal range of resistance values exists over which significant passive damping is added to a specific mode of the plate. Outside of this resistance interval the damping gradually reduces to zero. Shifting in the corresponding resonance frequency may also occur over this critical resistance range. The dependance of passive damping on the mode order, the type of piezoelectric material and the thickness of the piezoelectric layer was investigated. Overall, it was clearly illustrated that substantial vibration control of select modes can be obtained by proper configuration of the piezoelectric laminate and tuning of the resistive elements. Ongoing research is directed towards the development of approximate formulations for the analysis of damping in generalized curvilinear structures and the experimental verification of the piezoelectric damping concept.

ACKNOWLEDGMENT

Part of this work was performed under NASA cooperative agreement NCC3-391. This support is gratefully acknowledged.

REFERENCES

1. E. F. Crawley 1994 *AIAA Journal* **32**, 1689–1699. Intelligent structurs for aerospace: a technology overview and assessment.
2. S. S. Rao and M. Sunar 1994 *Applied Mechanics Reviews* **47**, 113–123. Piezoelectricity and its use in disturbance sensing and control of flexible structures: a survey.
3. N. W. Hagood and A. H. Von Flotow 1991 *Journal of Sound and Vibration* **146**, 243–268. Damping of structural vibrations with piezoelectric materials and passive electrical networks.
4. H. H. Law, P. L. Rossiter, G. P. Simon and L. L Koss 1996 *Journal of Sound and Vibration* **197**, 489–513. Characterization of mechanical vibration damping by piezoelectric materials.
5. C. L. Davis and G. A. Lesieutre 1995 *Journal of Sound and Vibration* **184**, 129–139. A modal strain-energy approach to the prediction of resistively shunted piezoceramic damping.
6. S. Koshigoe and J. W. Murdock 1993 *Journal of the Acoustical Society of America* **93**, 346–355. A unified analysis of both active and passive damping for a plate with piezoelectric transducers.

7. W. WANG K., J. S. LAI and W. K. YU 1996 *Journal of Vibration and Acoustics* **118** 505–509. An energy based parametric control approach for structural vibration suppression via semi-active piezoelectric networks.
8. S. YARLAGADDA, G. A. LESIEUTRE, S. YOSHIKAWA and J. WITHNAM 1996 *AIAA*-96-1291-*CP*, 37*th AIAA/ASME/ASCE/AHS/ASC SDM Conference and Adaptive Structures Forum*, *Salt Lake City*, *UT*. Resistively shunted piezocomposites for passive vibration damping.
9. H. F. TIERSTEN 1969, *Linear Piezoelectric Plate Vibrations*, New York: Plenum Press.
10. D. A. SARAVANOS 1997 *AIAA Journal* **35**, 1327–1333, Coupled mixed-field laminate theory and finite element for smart piezoelectric composite shell structures.
11. D. A. SARAVANOS, P. R. HEYLIGER and D. A. HOPKINS 1997 *International Journal of Solids and Structures* **34**, 359–378, Layerwise mechanics and finite element for the dynamic analysis of piezoelectric composite plates.

APPENDIX A: LAMINATE MATRICES

Stiffness matrices $[A]$, $[B]$, and $[D]$:

$$\begin{aligned}\langle A_{ij}, B_{ij}, D_{ij}\rangle &= \sum_{l=1}^{L}\int_{\zeta_l}^{\zeta_{l+1}} C_{ij}\langle 1, \zeta, \zeta^2\rangle \,\mathrm{d}\zeta, \quad i,j = 1, 2, 6,\\ A_{ij} &= \sum_{l=1}^{L}\int_{\zeta_l}^{\zeta_{l+1}} C_{ij}\,\mathrm{d}\zeta, \quad i,j = 4, 5.\end{aligned} \tag{A1}$$

Piezoelectric matrices $[\bar{E}^m]$ and $[\hat{E}^m]$

$$\begin{aligned}\langle \bar{E}^m_{ij}, \hat{E}^m_{ij}\rangle &= \sum_{l=1}^{L}\int_{\zeta_1}^{\zeta_{l+1}} e_{ij}\Psi^m_{,\zeta}(\zeta)\langle 1, \zeta\rangle \,\mathrm{d}\zeta, \quad i = 3, \quad j = 1, 2, 6,\\ \bar{E}^m_{ij} &= \sum_{l=1}^{L}\int_{\zeta_l}^{\zeta_{l+1}} e_{ij}\Psi^m(\zeta)\,\mathrm{d}\zeta, \quad i = 1, 2, \quad j = 4, 5.\end{aligned} \tag{A2}$$

Matrices of electric permittivity $[G^{mn}]$:

$$\begin{aligned}G^{mn}_{ii} &= \sum_{l=1}^{L}\int_{\zeta_l}^{\zeta_{l+1}} \varepsilon_{ii}\Psi^m(\zeta)\Psi^n(\zeta)\,\mathrm{d}\zeta, \quad i = 1, 2,\\ G^{mn}_{33} &= \sum_{l=1}^{L}\int_{\zeta_l}^{\zeta_{l+1}} \varepsilon_{33}\Psi^m_{,\zeta}(\zeta)\Psi^n_{,\zeta}\,\mathrm{d}\zeta.\end{aligned} \tag{A3}$$

Generalized densities ρ^A, ρ^B, ρ^D:

$$\langle \rho^A, \rho^B, \rho^D\rangle = \sum_{l=1}^{L}\int_{\zeta_1}^{\zeta_{l+1}} \rho_l\langle 1, \zeta, \zeta^2\rangle \,\mathrm{d}\zeta, \tag{A4}$$

where L is the number of plies in the laminate.